JOURNAL MATERIALS SCIENCE 14 (1979) 1651–1656

Operative slip systems in α–β brass two-phase bicrystals at 150 K

NABIL FAT-HALLA*
Graduate School, Tohoku University, Sendai, Japan

TAKAYUKI TAKASUGI, OSAMU IZUMI
The Research Institute for Iron, Steel and Other Metals, Tohoku University, Sendai, Japan

The study of the slip systems operated and activated at 3% strain in tension at 150 K has been carried out on α-β brass two-phase bicrystals and the role of the plastic incompatibility stresses is analyzed and discussed. Special emphasis has been given to the activation of the secondary slip which appeared near the phase-interface with respect to the elastic incompatible stresses. The results and other minor problems are discussed.

1. Introduction

Now that single crystal metals and alloys have been extensively studied, there is a need for a method to correlate the deformation characteristics of the single crystals with that of their polycrystalline materials. Over the last two decades, much research [1–9] has been carried out on bicrystals. The requirement of the plastic continuity at the grain boundary was first given by Livingston and Chalmers [1], and subsequently many authors [2–9] have rearranged and modified these formulae. Hook and Hirth [3] introduced the elastic incompatibility as an important factor controlling the deformation of bicrystals. Hirth has reviewed [5] the plastic and elastic requirements for the continuity of deformation at the grain boundary of bicrystals and he anticipated that the general anisotropic bicrystal case would give the result for interphase interfaces by analogy. Recently, the present authors prepared α-β brass two-phase bicrystals by means of the solid state diffusion couple method [10] and analysed the deformation [11] and fracture [12] behaviour of the bicrystal at room temperature.

Because the deformation behaviour of the b c c β brass is known to change drastically on lowering the temperature [13–17], which is not the case in f c c α brass [18–22], it was of interest to study the two-phase bicrystal at low temperatures. A temperature of 150 K was selected in order to avoid the occurrence of stress-induced martensitic transformation [23]. The present bicrystal components are known to possess a high degree of elastic anisotropy [24], hence special attention was given to the secondary slip systems which were activated near the phase-interface which is believed to result from the elastic incompatibility stresses.

2. Experimental procedures

The preparation of the α-β brass two-phase bicrystals has already been reported in detail [10]. The test temperature of 150 K was attained within ± 1.5 K through indirect cooling of the specimens.

Tensile specimens in which the phase-interface lies parallel to the tensile axis were spark-machined from the bicrystals with gauge dimensions of 18 mm length, 3 mm width and about 2 mm thickness. An Instron-type tensile testing machine was used at a strain-rate of 9.2×10^{-5} sec^{-1}. The specimens were deformed in tension up to about 3% plastic strain, then the slip traces were optically observed on two perpendicular surfaces to determine the slip planes. The orientations of both α and β phases before and after deformation were determined by the X-ray back-reflection Laue method. The stress and strain were calculated

---

* On leave from the Mechanical Department, Faculty of Engineering, Al Azhar University, Cairo, Egypt.

0022–2461/79/071651–06 $2.60/0

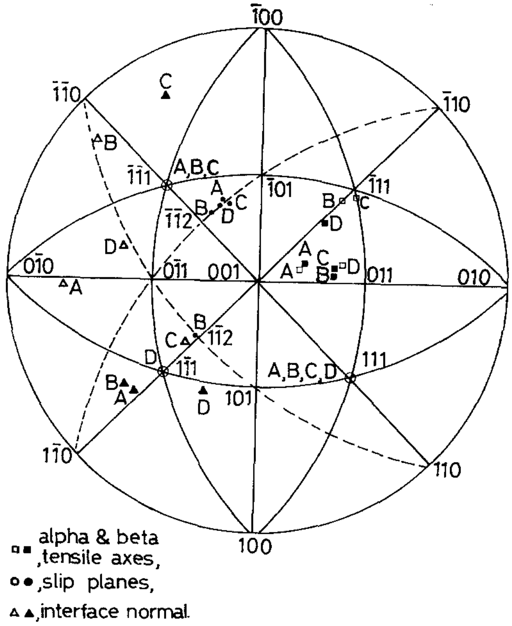

Figure 1 Stereographic analysis illustrating the tensile axes and the slip systems in both α and β components in a two-phase bicrystal.

with respect to the initial cross-section of the specimen and cross-head displacements, respectively.

3. Experimental results

Fig. 1 shows the orientations of both α and β phases in the various specimens with respect to the tensile axes. It can be seen that both the isoaxial* type specimen (A) and non-isoaxial type specimens (B to D) are included in the study.

The slip trace morphologies are shown in Figs. 2 and 3 for specimens A, and B, as typical examples. As can be seen, the general features of the α phase traces are well defined and straight, while those in the β phase are straight but weakly-defined. It is also obvious from the figures that although the conjugate slip is observed in both wide (XZ plane) and narrow (XY plane) faces in the α phases, as is schematically illustrated in Fig. 4, the primary slip is dominant. The slip traces on the β phase did not exhibit any conjugate slip in specimens A, C and D but conjugate slip was slightly observed in specimen B.

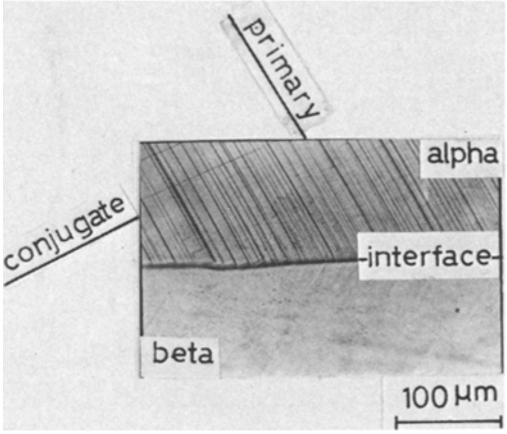

Figure 2 The slip trace morphology in both α and β phases of bicrystal 1 and 3% strain at 150 K.

Analysis of the slip traces on a stereographic projection in Fig. 1 revealed that in all specimens the primary $(1\,1\,1)[\bar{1}\,0\,1]$, in the α phase was operative. Specimens A to C showed conjugate slip of the type $(\bar{1}\,\bar{1}\,1)_\alpha[0\,1\,1]_\alpha$. The operation of this slip may be expected for specimen B or even C, since their tensile axes lie near the symmetry line $[0\,0\,1]$-$[\bar{1}\,1\,1]$ showing approximately equal Schmid factors for both the primary and conjugate systems, but it is not expected for specimen A. On the other hand, specimen D showed the cross-slip plane $(1\,\bar{1}\,1)$ at this strain (3%). These behaviours reflect the role of the plastic and/or elastic incompatibility stresses on the operative slip systems in the present two-phase bicrystal. The operative slip systems in the β phases are also illustrated in Fig. 1 showing that the primary slip planes lie on the great circle $[\bar{1}\,0\,1]$-$[\bar{1}\,\bar{1}\,2]$-$[0\,\bar{1}\,1]$ poles with the $[1\,1\,1]$ as the zone axis. The slip planes in the β phase have occupied variable positions (which cannot be considered as experimental error) along this great circle and this,

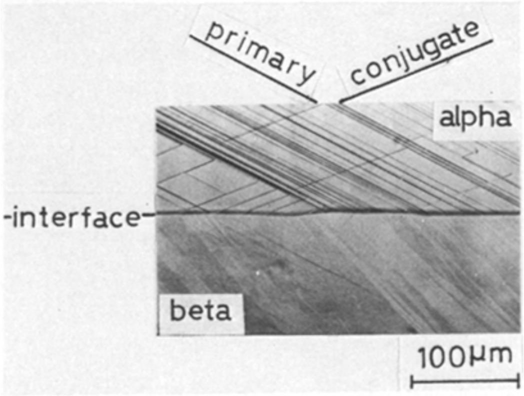

Figure 3 The slip trace morphology in both α and β phases of bicrystal 4 and 3% strain at 150 K.

---

* If the tensile axes, in both constituent phases, coincide with the same crystallographic direction in each component, the bicrystal is then defined as isoaxial.

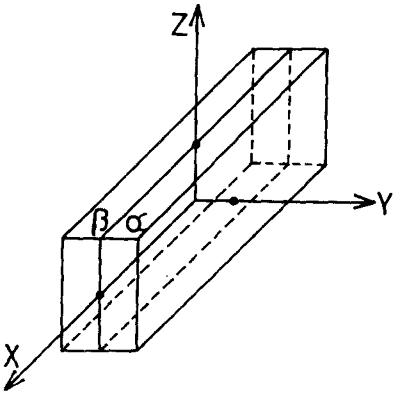

Figure 4 The geometry of the α-β brass two-phase bicrystal.

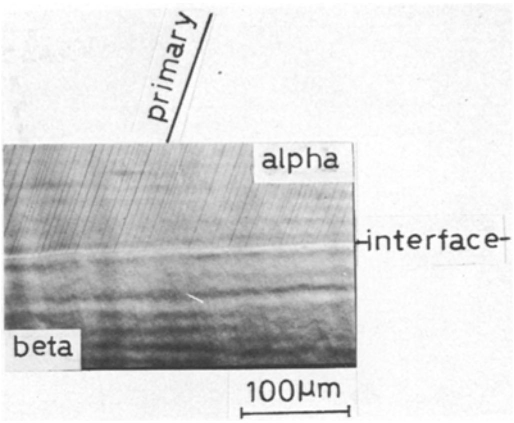

Figure 6 The disappearance of the secondary slip system due to the small value of elastic incompatibility.

again, reflects the effect of the two-phase interaction. Specimen B showed a conjugate slip plane laying along the great circle $[0\bar{1}1]$-$[1\bar{1}2]$-$[101]$ with zone axis $[\bar{1}11]$ at this strain (3%).

Furthermore, the secondary slip systems*, which were limited to zones near the interface and did not extend to the wide face of the specimens, were seen. In almost all the specimens, this activated secondary slip was observed but to different degrees. Fig. 5 shows the traces of this secondary system in the α phase as seen from the narrow face in specimen A, which exhibited the most remarkable traces of this type of slip. It is worthy of mention that specimen D did not show (or only very weakly seen in the optical microscope) this type of secondary slip near the interface, as can be seen from Fig. 6.

Fig. 7 shows the nominal stress–strain curves for the various specimens tensioned up to about 3% strain exhibiting different yield stresses and various strain-hardening rates; this will be discussed later.

4. Discussion

4.1. Plastic and elastic incompatibilities (basic equations)

The plastic deformation of the two-phase bicrystal shown in Fig. 4 requires both plastic and elastic continuity at the interface [5]:

$$\epsilon^{\alpha}_{xx} = \epsilon^{\beta}_{xx}, \quad \epsilon^{\alpha}_{zz} = \epsilon^{\beta}_{zz}, \quad \gamma^{\alpha}_{xz} = \gamma^{\beta}_{xz}, \tag{1}$$

where ϵ_{xx}, ϵ_{zz}, and γ_{xz} correspond to the plastic or elastic strains in each phase in the X, Z and XZ directions respectively. The plastic strain at the interface can be calculated assuming one constituent phase shears on slip system i by a unity. The three strain components of importance

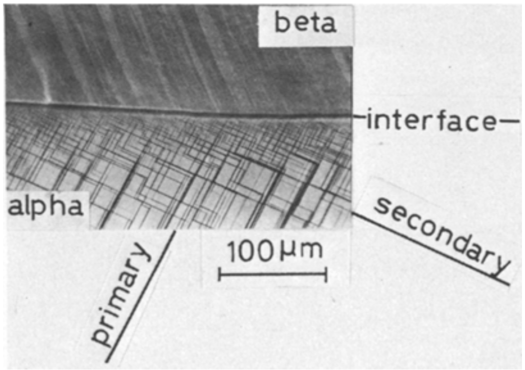

Figure 5 The clear existence of the secondary slip system near the interface in the α phase due to the elastic incompatibility.

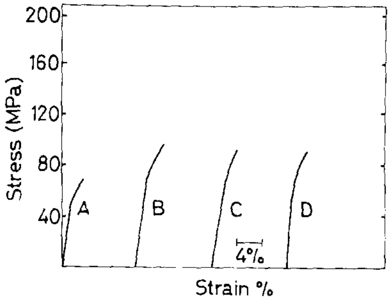

Figure 7 Stress–strain curves of the different two-phase bicrystals, the letters in the diagram indicate the specimen letters.

---

* The system that was activated near the interface and did not propagate up to the wide face will be called the "secondary system" in the present study.

TABLE I Plastic incompatibility strains

Specimen number	Slip systems Alpha	Slip systems Beta	$\Delta\epsilon_{xx}$	$\Delta\epsilon_{zz}$	$\Delta\gamma_{xz}$
A	$(111)[\bar{1}01]$	$(\bar{1}01)[111]$	0.027	0.089	0.034
	$(111)[\bar{1}01]$	$(\bar{1}\bar{1}2)[111]$	0.101	0.089	0.003
	$(111)[\bar{1}01]$	P_β [111]	0.079	0.118	0.020
B	$(111)[\bar{1}01]$	$(\bar{1}01)[111]$	0.151	0.399	0.302
	$(111)[\bar{1}01]$	$(\bar{1}\bar{1}2)[111]$	0.076	0.372	0.256
	$(111)[\bar{1}01]$	P_β [111]	0.101	0.383	0.269
C	$(111)[\bar{1}01]$	$(\bar{1}01)[111]$	0.138	0.072	0.099
	$(111)[\bar{1}01]$	$(\bar{1}\bar{1}2)[111]$	0.003	0.035	0.003
	$(111)[\bar{1}01]$	P_β [111]	0.084	0.004	0.020
D	$(111)[\bar{1}01]$	$(\bar{1}01)[111]$	0.050	0.065	0.015
	$(111)[\bar{1}01]$	$(\bar{1}\bar{1}2)[111]$	0.165	0.168	0.000
	$(111)[\bar{1}01]$	P_β [111]	0.099	0.148	0.034

at the interface are given by the following equations [3]:

$$\epsilon_{xx} = (e_i \cdot \mathbf{x})(g_i \cdot \mathbf{x}) \quad (2)$$

$$\epsilon_{zz} = (e_i \cdot \mathbf{z})(g_i \cdot \mathbf{z}) \quad (3)$$

$$\gamma_{xz} = \tfrac{1}{2}[(e_i \cdot \mathbf{x})(g_i \cdot \mathbf{z}) + (e_i \cdot \mathbf{z})(g_i \cdot \mathbf{x})], \quad (4)$$

where e_i and g_i are unit vectors in the directions normal to the slip plane and parallel to the slip direction, respectively, **x** and **z** are unit vectors in the X and Z directions illustrated in Fig. 4.

The elastic strain can be calculated in the X, Z and XZ directions of the bicrystal using the following equations published by Smithells [24]:

$$\epsilon_{ij} = \frac{1}{E} \cdot \sigma = \{S_{11} - 2[(S_{11} - S_{12}) - \frac{1}{2}S_{44}] \times (l^2m^2 + m^2n^2 + n^2l^2)\}\sigma \quad (5)$$

$$\gamma_{ij} = \frac{1}{G} \cdot \tau = \{S_{44} - 2[(S_{11} - S_{12}) - \frac{1}{2}S_{44}] \times (l^2m^2 + m^2n^2 + n^2l^2)\}\tau, \quad (6)$$

where S_{ij} represents the standard compliances of the component single crystals, l, m and n are the direction cosines of the specified direction with respect to that of the crystallographic axes.

Thus the plastic and elastic incompatible strains as previously indicated [11], can be given by:

$$\Delta\epsilon_{xx} = |\epsilon^{\alpha}_{xx} - \epsilon^{\beta}_{xx}| \quad (7)$$

$$\Delta\epsilon_{zz} = |\epsilon^{\alpha}_{zz} - \epsilon^{\beta}_{zz}| \quad (8)$$

$$\Delta\gamma_{xz} = |\gamma^{\alpha}_{zz} - \gamma^{\beta}_{zz}|. \quad (9)$$

Equations 7 to 9 were used to calculate the plastic incompatible strains given in Table I and the elastic incompatible strains in Table II.

4.2. Discussion of the present results

The deformation of α brass single crystals was extensively studied over wide range of temperatures, strain-rates and strains [18–22, 25]. The essence of these results indicates that the operating slip system at 150 K is $(111)[\bar{1}01]$ when the tensile axis lies inside the standard triangle [001]-[011]-$[\bar{1}11]$; the CRSS on this operating system was determined as 20.6 MN m^{-2} at 150 K. On the other hand, the deformation of the β brass single crystals (near the stoichiometric composition) was studied at low temperatures [13–17, 26–30]. The literature results show that the slip plane observed at low temperatures depends on both the test temperature and the orientation. This slip plane always lies on the great circle $[\bar{1}01]$-$[\bar{1}\bar{1}2]$-$[0\bar{1}1]$ between the first two poles with the zone axis (slip direction) coinciding with the [111] pole. The previously observed slip system [13, 16] at 77 K was the $(\bar{1}\bar{1}2)[111]$. However, the deviation of the observed slip plane from the $(\bar{1}01)$ towards $(\bar{1}\bar{1}2)$ at the present temperature of 150 K is still a matter for argument.

The present results on the α phases show, in all the specimens tested, the operation of the primary $(111)[\bar{1}01]$ slip system which is expected from the behaviour of the α brass single crystals. The appearance of the conjugate systems $(\bar{1}\bar{1}1)$ [011] and the cross-slip systems $(1\bar{1}1)$ in all

TABLE II Elastic strain incompatibility × 10^{-9}

Specimen number	$\Delta\epsilon_{xx}$	$\Delta\epsilon_{zz}$	$\Delta\gamma_{xz}$
A	0.12	0.13	0.11
B	0.11	0.12	0.10
C	0.13	0.06	0.14
D	0.09	0.10	0.10

the specimens, can be explained for specimens B and C on the basis of nearly equal Schmid factors for both the primary and conjugate systems in the α phase. On the other hand, the existence of the conjugate slip systems in the α components A and D can only be explained on the basis of the incompatible stresses as follows: referring to Fig. 7, it is observed that at stresses of about 42.1 and 44.1 $\mathrm{MN\,m^{-2}}$ the value of the RSS on the primary slip systems in the α phases of specimens 1 and 4, respectively, has reached its critical value (20.6 $\mathrm{MN\,m^{-2}}$). The deformation can continue on this system only if the α component is deformed solely. Since the CRSS was not yet reached in the β phase at this level of stress, the deformation of the β components continues elastically while that in α phases procedes plastically. Although a detailed analysis of the bicrystal in the elastic–plastic state is not yet available, this situation results in a high rate of stress increase in the α phase which is not comparable to that observed in the deformation of α brass single crystals. Moreover, it is believed that the CRSS value on the conjugate systems in the α phases, being $(\bar{1}\,\bar{1}\,1)$ $[0\,1\,1]$ for specimens A and C, and $(1\,\bar{1}\,1)[\bar{1}\,0\,1]$ for specimen D, was reached at the stress levels attained at 3% strain. Hence, it is noted that the incompatibility between the two component crystals resulted in the appearance of conjugate slip systems in the α phases which was not expected from the deformation of α brass single crystals at the same strain.

The present results on the β components of the bicrystals indicate, as shown in Fig. 1, the operation of the primary slip systems with the $[1\,1\,1]$ as the slip direction and slip planes P_β (P_β is defined as the actual observed slip plane) between the $[\bar{1}\,0\,1]$ and $[\bar{1}\,\bar{1}\,2]$ poles. Considerable attention has been paid to the deviation of P_β in the β brass single crystals from the slip plane predicted theoretically [26] and observed experimentally at low temperatures [15, 16, 28, 29]. Although a concrete theory has not yet been established, there is strong indication that the deformation of the β brass single crystals at low temperatures is generally controlled by the operation of cross-slip. In the present research in which β brass contains about 41% zinc and is tested at 150 K, it is believed that the parameters [29] controlling the cross-slip operation change in such a way as to facilitate the occurrence of cross-slip. It is to be noted that the deformation of the β component has proceeded partially by the previously mentioned cross-slip operation resulting in a macroscopical slip plane P_β lying between $(\bar{1}\,0\,1)$ and $(\bar{1}\,\bar{1}\,2)$. Now we can discuss why the P_β occupies different locations on the $(\bar{1}\,0\,1)$-$(\bar{1}\,\bar{1}\,2)$-$(0\,\bar{1}\,1)$ great circle with respect to the plastic incompatible strains. It should be noted that both the applied stress and the plastic incompatible stresses are acting on each component crystal. Referring to Table I listing the calculated values of the incompatible plastic strains, it is noticed that in specimens A to C the incompatibility between the two systems $(1\,1\,1)_\alpha[1\,0\,1]_\alpha$ and $(\bar{1}\,\bar{1}\,2)_\beta[1\,1\,1]_\beta$ is at an optimum value. It is believed in the present study that the value of the incompatibility stress alters the position of P_β at which the total applied stress[†] reaches the value of the CRSS; in other words if the incompatible stress value (measured by the incompatible strain) is high then P_β will occur nearer to the $(\bar{1}\,\bar{1}\,2)$ and vice versa. It is clear from Table I that specimen B exhibits the highest plastic incompatibility and that its position is the nearest to the $(\bar{1}\,\bar{1}\,2)$ plane. Although the best degree of compatibility in specimen D was found to be between $(1\,1\,1)_\alpha[\bar{1}\,0\,1]_\alpha$ and $(\bar{1}\,0\,1)_\beta[1\,1\,1]_\beta$, movement of P_β towards the $(\bar{1}\,0\,1)_\beta$ plane could not be detected owing to the high CRSS in this direction [13, 16, 17].

Of special interest to the present research is the activation of the secondary slip systems near the interface, since the present bicrystal is two-phase, with a high degree of elastic anisotropy[†]. The

---

[*] The total applied stress is defined as the resultant of the externally applied stress and the incompatible stress both resolved on the operative slip system.

[†] Using the values given for the standard compliances for both α brass single crystals [31] and β brass single crystals [32] at low temperatures and using the equation published previously [24], the degree of elastic anisotropy, being equal to

$$\frac{2(S_{11}-S_{12})}{S_{44}},$$

is estimated for α and β brasses in the present study to be 4 and 10.9, respectively (it is to be noted that the corresponding factor for isotropic material is 1).

elastic incompatible strains $\Delta\,\epsilon_{xx}$, $\Delta\,\epsilon_{zz}$ and $\Delta\,\gamma_{xz}$, were calculated from Equations 7 to 9 and the results are summarized in Table II which indicates that specimen A had the highest value of incompatible elastic strain. Although a detailed analysis of the secondary slip could not be obtained owing to the short penetration of this system, it is clear from Fig. 5 that the strong existence of this secondary slip is observed in specimen A (the most remarkable occurrence). Fig. 6 showed that for specimen D with low elastic incompatibility strains (Table II) this secondary system could not be observed on either of the narrow sides. Hence, it can be concluded that these activated systems near the interface are due to the elastic incompatibility between the two constituent phases. Further study in this area is needed to clarify the secondary systems which were activated near the interface.

5. Conclusions

(1) In all α-β brass two-phase bicrystals tested, the primary $(1\,1\,1)_\alpha[\bar{1}\,0\,1]_\alpha$ system, in the α phases, and the primary $P_\beta[1\,1\,1]_\beta$, in the β phases were operative in tension at 150 K (P_β being the actual observed slip plane in the β phase lying between $[\bar{1}\,0\,1]$ and $[\bar{1}\,\bar{1}\,2]$).

(2) The conjugate and secondary slip systems were activated in the α phases due to plastic and elastic incompatibilities between the component crystals at this small strain (3%). The slip systems introduced by the former type of compatibilities extended into the matrix far from the interface, while those introduced by the latter type were restricted to near the interface.

(3) The role played by the elastic incompatible strains could be clarified by calculating the values for the different bicrystals and correlating these values with the experimentally observed secondary slip near the interface.

Acknowledgement

One of the authors (N.F.) wishes to express his pleasure and thanks to Dr. S. Hanada for his fruitful discussions and constructive criticism through out this research.

References

1. J. D. LIVINGSTON and B. CHALMERS, *Acta Met.* 5 (1957) 322.
2. J. J. HAUSER and B. CHALMERS, *ibid* 9 (1961) 802.
3. R. E. HOOK and J. P. HIRTH, *ibid* 15 (1967) 535.
4. *idem, ibid* 15 (1967) 1099.
5. J. P. HIRTH, *Met. Trans.* 3 (1972) 3047.
6. Y. CHUANG and H. MARGOLIN, *ibid* 4 (1973) 1905.
7. T. D. LEE and H. MARGOLIN, *ibid* 8A (1977) 157.
8. A. K. HINGWE and K. N. SUBRAMANIAN, *J. Mater. Sci.* 10 (1975) 183.
9. U. F. KOCKS, *Phil. Mag.* 10 (1964) 187.
10. T. TAKASUGI, N. FAT-HALLA and O. IZUMI, *J. Mater. Sci.* 13 (1978) 2013.
11. *idem, Acta Met.* 26 (1978) 1453.
12. N. FAT-HALLA, T. TAKASUGI and O. IZUMI, *J. Mater. Sci.* 13 (1978) 2462.
13. S. HANADA, M. MOHRI and O. IZUMI, *Trans. JIM* 16 (1975) 453.
14. G. W. ARDLEY and A. H. COTTRELL, *Proc. Roy. Soc.* A219 (1953) 328.
15. N. BROWN, *Phil. Mag.* 4 (1) (1959) 693.
16. M. YAMAGUCHI and Y. UMAKOSHI, *Acta Met.* 24 (1976) 1061.
17. Y. YAMAGATA, H. YOSHIDA and Y. FUKUZAWA, *Trans. JIM* 17 (1976) 393.
18. R. MADDIN, C. MATHEWSON and W. HIBBARD, *Met. Trans. (AIME)* 185 (1949) 527.
19. R. E. JAMISON and F. A. SHERRILL, *Acta Met.* 4 (1956) 197.
20. P. R. THORNTON and T. E. MITCHELL, *Phil. Mag.* 7 (1962) 361.
21. T. E. MITCHELL and P. R. THORNTON, *ibid* 8 (1963) 1127.
22. H. TRAUB, H. NEUHAUSER and C. H. SCHWINK, *Acta Met.* 25 (1977) 437.
23. M. AHLERS, R. PASCUAL and R. RAPACIOLI, *Mat. Sci. Eng.* 27 (1977) 49.
24. C. J. SMITHELLS, “Metals Reference Book”, 5th Edn., (Butterworths, London and Boston, 1976), pp. 975–9.
25. P. R. THORNTON, T. E. MITCHELL and P. B. HIRSCH, *Phil. Mag.* 7 (1962) 1394.
26. D. I. POTTER, *Mat. Sci. Eng.* 5 (1969/1970) 201.
27. W. A. RACHINGER and A. H. COTTRELL, *Acta Met.* 4 (1956) 109.
28. M. M. SHEA and N. STOLOFF, *Mat. Sci. Eng.* 12 (1973) 245.
29. H. M. CLARK, *Phil. Mag.* 16 (1967) 853.
30. A. L. TITCHER and W. G. FERGUSON, *J.I.M.* 99 (1971) 345.
31. J. A. RAYNE, *Phys. Rev.* 115 (1959) 63.
32. G. M. MCMANUS, *ibid* 129 (1963) 2004.

Received 6 September and accepted 12 October 1978.